BMC Genomics

RESEARCH

Open Access

High temporal-resolution transcriptome landscape reveals the biological process and regulatory genes of melanin deposition in breast muscle of Silkie chickens during embryonic development

Xinting Yang[1†], Bowen Ma[1†], Qingyu Zhao[1], Yaxiong Jia[1], Qingshi Meng[1], Yuchang Qin[1], Chaohua Tang[1*] and Junmin Zhang[1*]

Abstract

Background Abnormal deposition of melanin in skeletal muscle is an interesting phenomenon and the Silkie is the most typical example. Melanin deposition involves multiple steps such as neural crest cell migration, melanocyte differentiation, melanosome assembly and melanin biosynthesis, which have already occurred during the embryonic stage of Silkies. However, there is no comprehensive understanding of the dynamic changes in the biological processes and regulatory mechanism underlying melanin deposition in skeletal muscle during chicken embryonic development.

Results In this study, high-performance liquid chromatography (HPLC) was used to accurately measure the melanin content in breast muscle across 13 embryonic time points. There was no melanin in breast muscle on embryonic day 8 (E08) to E10, a trace amount of melanin on E11 to E16 and a large amount of melanin on E17 to E21. According to melanin content and deposition pattern, the melanin deposition process in breast muscle was further divided into five stages, including E08 to E10, E11 to E14, E15 to E16, E17 to E18, and E19 to E21. High temporal-resolution transcriptome analysis was performed in the breast muscle of Silkies across 13 embryonic time points. The protein-coding genes (PCGs) and transcriptional factors (TFs) significantly specifically expressed at these five stages were identified. Among these stage-specific genes, stage-specific DEGs between Silkies and Wenchang chickens without melanosis were further screened at each stage. During E08 to E10, three stage-specific DEGs and one stage-specific TF act on neural crest cell migration and melanocyte stem cell differentiation. During E17 to E21, nine stage-specific DEGs and one stage-specific TF act on melanosome assembly and melanin biosynthesis. During E19 to E21, one stage-specific DEG enhances melanin biosynthesis. These stage-specific DEGs and TFs all affect the final melanin content of breast muscle.

[†]Xinting Yang and Bowen Ma contributed equally to this work.

*Correspondence:
Chaohua Tang
tangchaohua@caas.cn
Junmin Zhang
zhangjunmin@caas.cn

Conclusions This study reveals the critical stage of melanin deposition in breast muscle during the embryonic development, and identified the biological processes and functional genes at each stage. This study provides novel insights into the biological process and regulatory mechanism of melanin deposition in skeletal muscle and provides a reference for breeding Silkies with high muscle melanin content.

Keywords Silkie chicken, Breast muscle, Melanin deposition, Embryonic development, Transcription regulation

Background

Melanin is widely distributed in the epidermis, hair follicles, choroid, iris, inner ear and other tissues of vertebrates [1]. However, abnormal melanin deposition has also been found in the dermis, connective tissue and skeletal muscle of some chicken breeds [2]. The Silkie, renowned for its snow-white feathers and black skin, muscles, and bones, is recorded as an ancient and famous chicken breed in The Travels of Marco Polo. The Silkie is the most widespread and well-studied breed displaying this phenomenon and this trait is due to their sex-linked Inhibitor of Dermal Melanin (*ID*) and Fibromelanosis (*FM*) mutations. The *ID* mutation located on the Z chromosome can cause abnormal migration of neural crest cells [3]. The *FM* mutation is caused by repetition and inversion of the genome segment containing *EDN3* [2], which not only enhances the yield of melanoblasts specified from neural crest cells, but also further drives their maturation [4]. Melanoblasts can further differentiate into melanocytes; melanosome assembly is completed within melanocytes and melanin biosynthesis occurs within the melanosomes. This complex biological process occurs in Silkies during the embryonic period. Existing studies primarily compared light and dark black-boned chickens at a single time point after birth [5–8], and one study examined the differences between black-boned and non-black-boned chickens during the embryonic period [9]. However, there is no comprehensive understanding of the dynamic changes in the biological processes and regulatory mechanism underlying melanin deposition in skeletal muscle during chicken embryonic development. The melanin content in Silkies muscle continues to decrease after birth (Fig. S1), and therefore, studying the regulatory mechanism of melanin deposition during the embryonic period is crucial to increasing the melanin content.

Gene expression is spatiotemporally specific and genes expressed stage-specifically during development often have some physiological functions. A study on sheep hair follicular development showed that protein-coding genes (PCGs) with stage-specific expression or regulated by stage-specific long non-coding RNAs, microRNAs and circular RNAs were significantly enriched in epithelial differentiation and hair follicle morphogenesis [10]. A study on transcriptome analysis of two pig breeds across 27 time points found that Landrace showed a developmental lag and stronger myoblast proliferation and cell migration, but Tongcheng had higher ATP synthase activity in postnatal periods [11].

This study used high-performance liquid chromatography (HPLC) to measure the melanin content in the breast muscle of Silkies across 13 embryonic time points and determined the melanin distribution and deposition pattern in breast muscle through Hematoxylin and Eosin (HE) and Fontana-Masson (FM) staining. Based on the melanin content and deposition pattern, the melanin deposition process of breast muscle was divided into five stages. High temporal-resolution transcriptome landscapes of breast muscle in Silkies across 13 embryonic time points were generated, which identified stage-specific PCGs and transcriptional factors (TFs) at these five stages. Among these stage-specific genes, stage-specific differentially expressed genes (DEGs) between Silkie and Wenchang chickens without melanosis were identified at each critical stage. The Gene Ontology (GO) enrichment analysis of these stage-specific DEGs was performed to reveal the physiological changes in skeletal muscle associated with melanin deposition process. Finally, the stage-specific DEGs and TFs that play a direct role in melanin deposition of breast muscle were identified at each stage, and the effects of these stage-specific DEGs and TFs on melanin content were verified in breast muscle of adult Silkies. This study provides novel insights into the occurrence period, biological process and regulatory genes of melanin deposition in breast muscle during embryonic development and provides a research basis for breeding Silkies with a high melanin content in breast muscle.

Results

Melanin deposition pattern in breast muscle during embryonic development

To explore the dynamic change of melanin deposition in breast muscle during embryonic development, HPLC was used to measure the melanin content in the breast muscle across 13 embryonic time points (embryonic day 8 (E08), E09, E10, E11, E12, E13, E14, E15, E16, E17, E18, E19 and E21) and 3 male chicken embryos at each time point (Fig. 1-A; Table S1). Analysis of variance showed significant differences in the melanin content among the

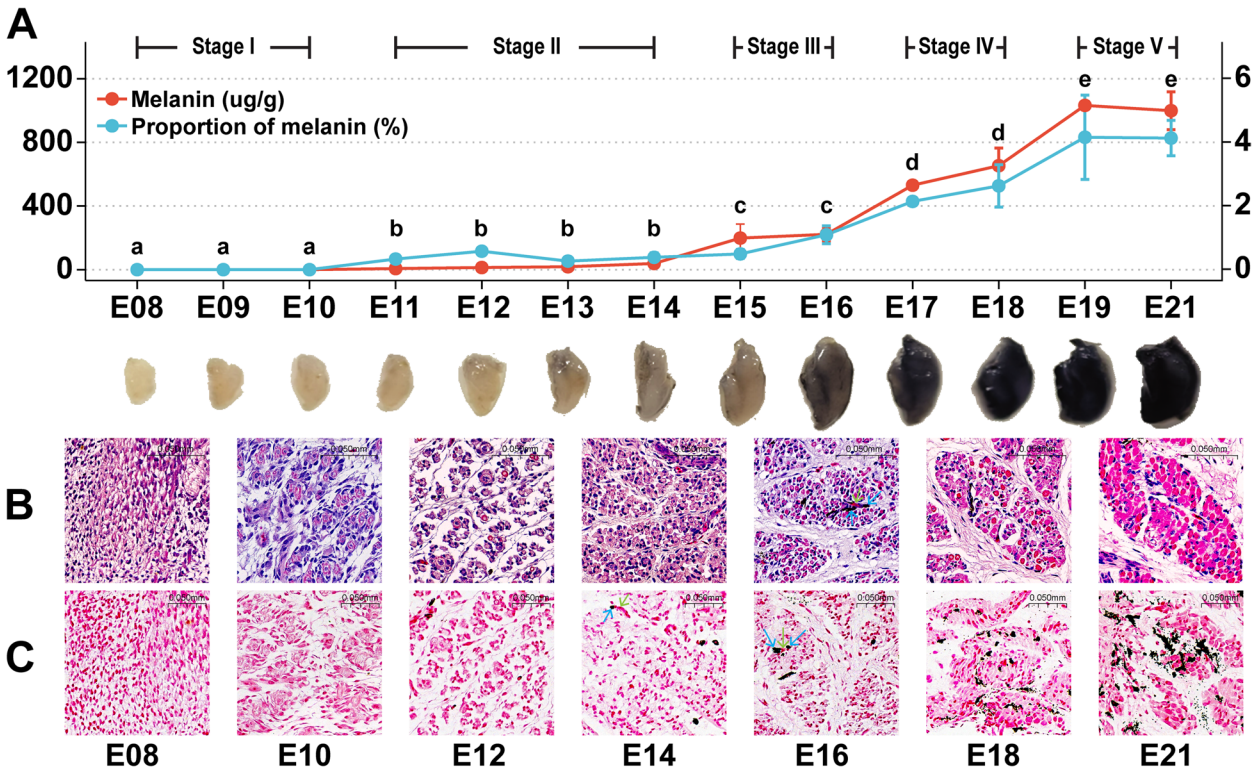

Fig.1 The melanin deposition patterns and histomorphology observation of breast muscle in Silkies across 13 time points during the embryonic period. **A** Changes in melanin content during breast muscle development. The red line is melanin content detected by HPLC, and the blue line is the statistical proportion of melanin granules by FM staining. Data with different letters on each bar mean statistically significant difference among time points ($p < 0.05$). **B** HE staining of transversal breast muscle sections. **C** FM staining of transversal breast muscle sections. The green arrow points to blood cells, and the blue arrow points to melanin

five stages, including E08 to E10, E11 to E14, E15 to E16, E17 to E18, and E19 to E21.

Transversal sections of breast muscle were stained by HE (Fig. 1-B) and FM (Fig. 1-C) to observe the histological changes and melanin deposition patterns during breast muscle development. During E08 to E09, a large number of free unfused myoblasts were present. At this time, melanin granules have not yet appeared and the melanin content could not be detected. At E10, myoblasts began to differentiate. During E11 to E14, a large number of myoblasts fused into primary multinucleated myotubes, which were round and had nuclei within and around them. At this time, sporadic melanin granules appeared around primary multinucleated myotubules and blood cells and trace amounts of melanin could be measured. During E15 to E16, the myofibril in myotube gradually increased, causing the nuclei in myotubes to gradually move toward the periphery of cells, becoming what are called secondary myotubes. The perimysium began to thicken significantly and melanin granules began to accumulate on the perimysium and around blood vessels. During E17 to E19, the nuclei in myotube moved completely to the periphery of cell and fusion was enhanced to form muscle fibers. The distribution of melanin granules gradually increased and the track of transport along the perimysium to the fasciculus could be clearly seen. During this stage, the melanin content increased dramatically and reached its maximum by E19. At E21, myofibrils filled the interior of the cell, the nuclei were pushed to the very edge and the muscle fibers matured and thickened in diameter, with the melanin content at its highest level. According to the changes in melanin content and deposition pattern, the melanin deposition process of breast muscle was divided into five stages, including E08 to E10, E11 to E14, E15 to E16, E17 to E18, and E19 to E21.

Identification of stage-specific genes in breast muscle during embryonic development

The PCA based on all transcripts revealed that the developmental stage was the major factor distinguishing samples (Fig. 2-A). This study identified genes specifically expressed in five stages, where 1614, 517, 100, 936 and 1901 genes were significantly upregulated, while 2462, 1852, 463, 1070 and 2712 genes were significantly downregulated at stage I, stage II, stage III, stage IV and stage

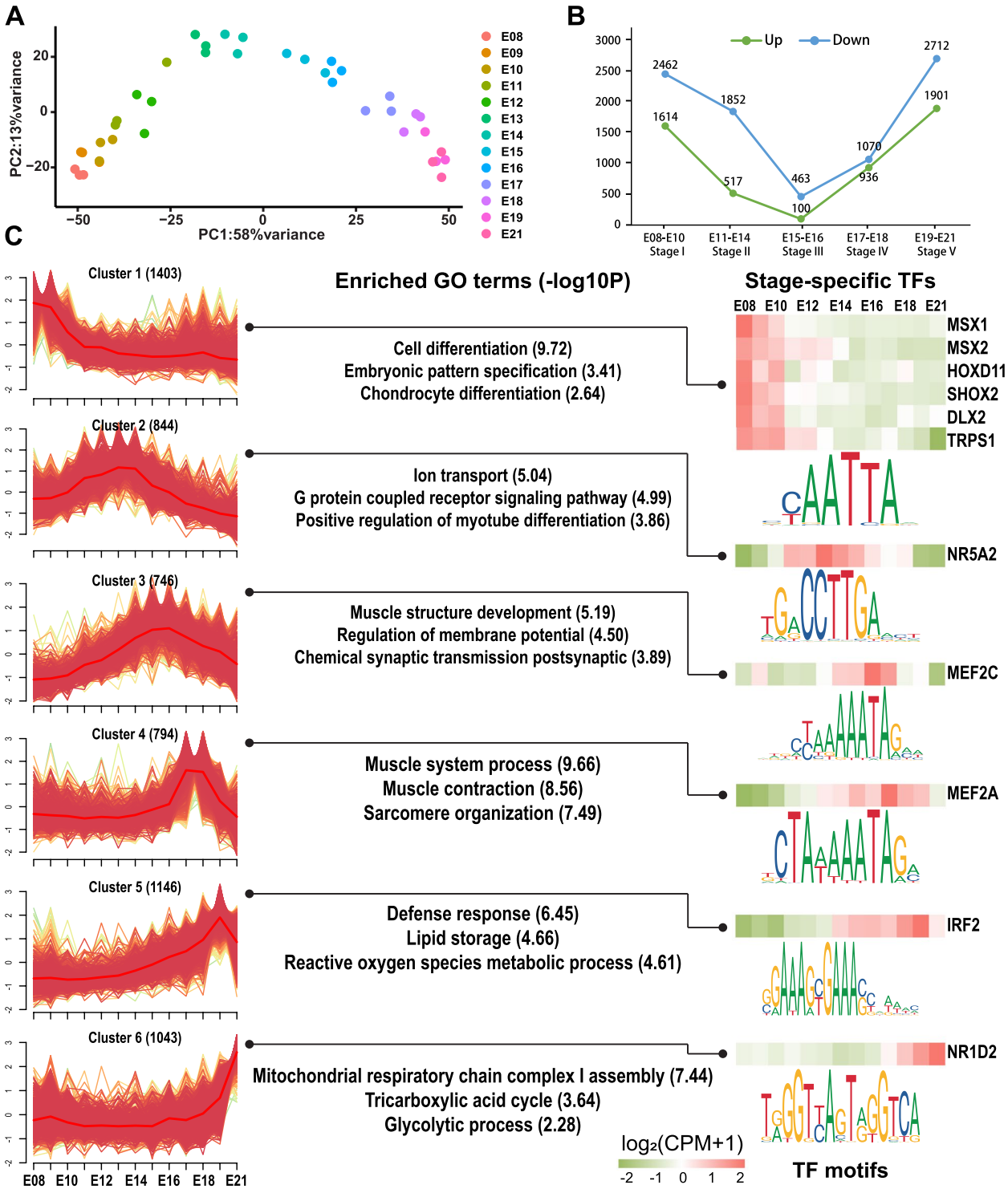

Fig.2 Identification of stage-specific genes during breast muscle development. **A** PCA based on all transcripts. **B** Numbers of stage-specific genes during breast muscle development. Green lines: upregulation; blue lines: downregulation. **C** K-means clusters of all stage-specific genes. Top enriched GO terms (biological process; BP), and the top representative motifs of TFs in each cluster are shown next to each cluster

V (Fig. 2-B). The upregulated and downregulated stage-specific genes were grouped into six clusters with different expression trends across stages (Fig. 2-C, Table S2). To investigate whether stage-specific PCGs in each cluster were co-regulated by certain TFs, a motif enrichment analysis was performed on the promoters, located 1500 bp up- and 500 bp downstream of transcription start sites (TSS) of PCGs in each cluster (Table S3). The expression trend of target TFs was consistent with that of stage-specific PCGs which belonged to the same cluster, indicating that these TFs might play vital roles during embryonic breast muscle development.

The PCGs and TFs in six clusters exhibited distinct biological functions (Fig. S2; Table S4). The PCGs in cluster1 showed the highest expression levels at E08 to E10 and were significantly enriched in embryonic pattern specification and chondrocyte differentiation ($p < 0.01$). Their promoters were significantly enriched for motifs of TFs which played important roles in pattern formation during development, including *MSX1, MSX2* and *SHOX2*, and chondrocyte proliferation and differentiation-related TFs, including *SOX9* and *TRPS1*. The PCGs in cluster2 were highly expressed at E11 to E14 and were significantly enriched in ion transport ($p < 0.01$). The PCGs in cluster3 were highly expressed at E15 to E16 and were significantly enriched in muscle structure development and chemical synaptic transmission ($p < 0.01$). Their promoters were significantly enriched for motifs of *MEF2 C*, which played a key role in evoking synaptic transmission. The PCGs in cluster4 were highly expressed at E17 to E18 and were significantly enriched in muscle system process and muscle contraction ($p < 0.01$). Their promoters were significantly enriched for motifs of *MEF2 A*, which is involved in muscle development. The PCGs in Cluster5 showed the highest expression levels at E19 and were significantly enriched in defense response and reactive oxygen species metabolic process ($p < 0.01$). The PCGs in Cluster6 showed the highest expression levels at E21 and were significantly enriched in the tricarboxylic acid cycle and glycolytic process ($p < 0.01$). Their promoters were significantly enriched for motifs of *NR1D2*, which regulated energy homeostasis.

The change of genes and pathways caused by melanin deposition in breast muscle during embryonic development

In order to explore the genes and pathways related to melanin deposition process, the stage-specific DEGs between Silkies and Wenchang chickens were further screened among the genes specifically expressed in five stages (Fig. 3-A; Table S5), and GO enrichment analysis of these stage-specific DEGs was performed (Fig. 3-B). A total of 78 genes with stage-specific expression at E09 were differentially expressed between Silkies and Wenchang chickens, and significantly enriched in positive regulation of mesenchymal cell proliferation, collagen-containing extracellular matrix, vasoconstriction, neural crest cell migration and positive regulation of collagen biosynthetic process. A total of 70 genes with stage-specific expression at E13 were differentially expressed between Silkies and Wenchang chickens, and significantly enriched in ATPase-coupled transmembrane transporter activity, postsynaptic neurotransmitter receptor diffusion trapping, endothelial cell chemotaxis, cell migration involved in sprouting angiogenesis and neural crest cell development. A total of 169 genes with stage-specific expression at E17 were differentially expressed between Silkies and Wenchang chickens, and significantly enriched in melanosome membrane, melanin biosynthetic process, melanosome organization, melanocyte differentiation and developmental pigmentation. A total of 84 genes with stage-specific expression at E21 were differentially expressed between Silkies and Wenchang chickens, and significantly enriched in mitochondrial respiratory chain complex I assembly, aerobic respiration, cholesterol homeostasis, removal of superoxide radicals and mitochondrial respiratory chain complex III assembly.

Identification of stage-specific DEGs and TFs with crucial roles in breast muscle melanin deposition process

We further screened 19 melanin-related key genes among the stage-specific DEGs between Silkies and Wenchang chickens (Fig. 4-A). Of these, *SOX9, PAX3, KIT, EDN3* and *EDNRB2* with stage-specific expression at E9, *SOX10, SLC45 A2, OCA2, TRPM1, RAB38, MLPH, MC1R, TYRP1, PMEL, MLANA, GPNMB* and *DCT* with stage-specific expression at E17, and *GPR143* and *STAP2* with stage-specific expression at E21 were all significantly highly expressed in Silkies.

To investigate whether these 19 melanin-related stage-specific DEGs were collectively regulated by certain TFs, a motif enrichment analysis was performed on their promoters and 16 TFs were detected (Fig. 4-B; Table S6). These TFs exhibited stage-specific expression consistent with target DEGs, indicating they might play vital roles in melanin deposition process. Figure 4-C and Table S7 showed the regulatory relationship between TFs and target melanin-related DEGs, where *TFAP2 A* and *TFAP2B* showed stage-specific expression at E08 and E09 and acted as central TFs promoting melanoblast differentiation, positively regulated *EDN3, EDNRB2* and *KIT* with Pearson correlation coefficient (PCC) exceeding 0.6. The *MITF* showed stage-specific expression at E17 to E21 and played an important role in melanocyte development, positively regulating *DCT, GPNMB, MLANA,*

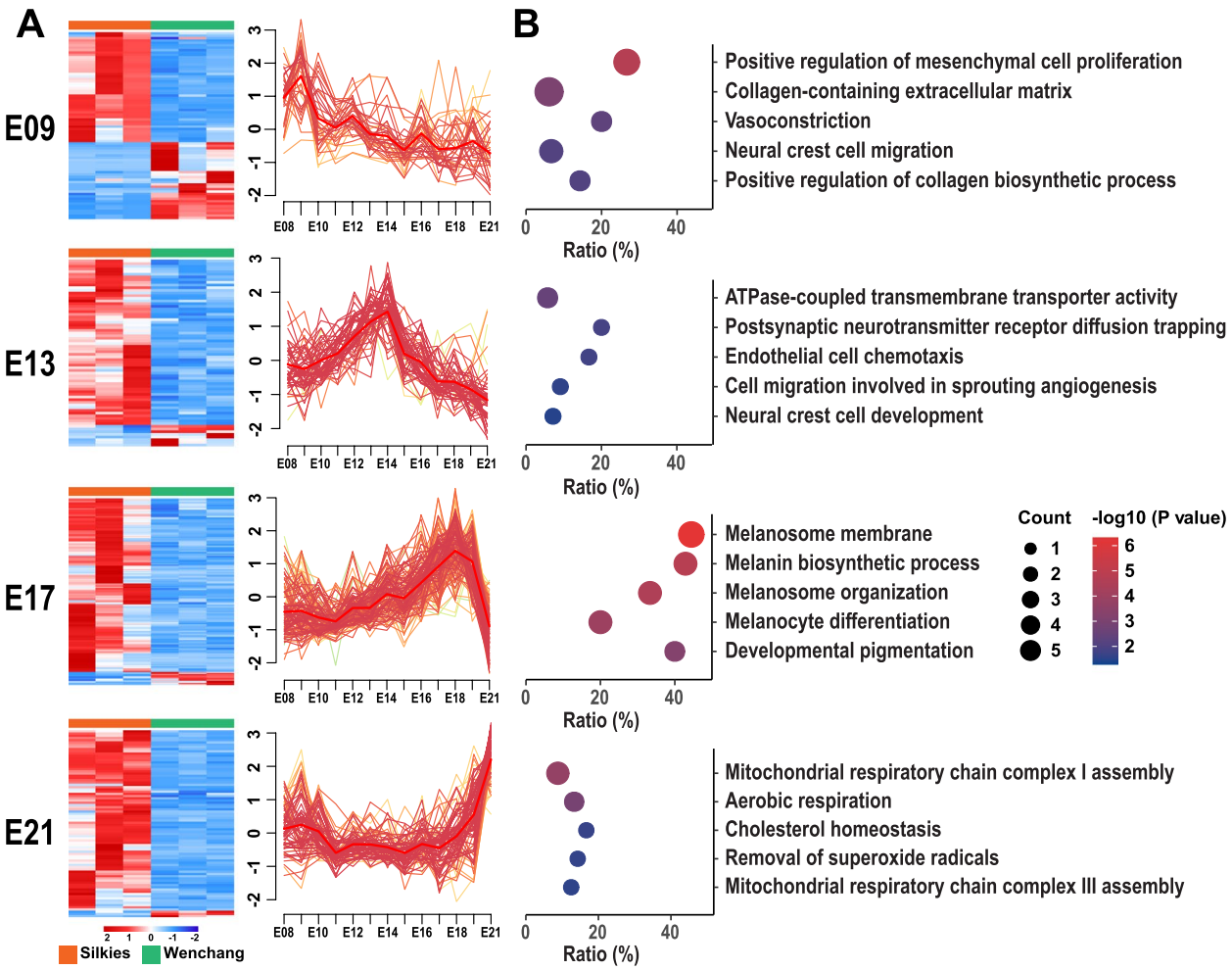

Fig.3 Identification and GO enrichment analysis of stage-specific DEGs between Silkies and Wenchang chickens. **A** The Identification and K-means clustering of stage-specific DEGs between Silkies and Wenchang chickens at various stages of melanin deposition. **B** The significantly enriched GO terms for stage-specific DEGs

MLPH, OCA2, SLC45 A2, SOX10, STAP2, TRPM1, TYRP1 and *PMEL* with PCC exceeding 0.6.

The functions of stage-specific DEGs and TFs in melanin deposition process and their effects on breast muscle melanin content

The detailed functions of these stage-specific DEGs in the melanin deposition process were showed in Fig. 5. The DEGs with stage-specific expression at E08 to E10 play key roles in neural crest cell migration and melanocyte stem cell differentiation, DEGs with stage-specific expression at E17 to E21 mainly play key roles in melanosome assembly and melanin biosynthesis, and the DEGs with stage-specific expression at E21 mainly assist melanin biosynthesis.

In order to explore the impact of these two critical stages, including E08 to E10 and E17 to E21, on the final melanin content, the melanin content and the expression levels of stage-specific DEGs and TFs were detected in breast muscle of adult Silkies. It was found that three DEGs and one TF with stage-specific expression at E08 to E10 and 10 DEGs and one TF with stage-specific expression at E17 to E21 were significantly correlated with the final melanin content in breast muscle (Fig. 6; Table S8), indicating that the processes of melanocyte differentiation, melanosome assembly and melanin biosynthesis were all crucial for the final melanin content.

Discussion

Abnormal melanin deposition in the skeletal muscle of Silkies is an interesting phenomenon and this complex process begins during the embryonic period. Existing studies primarily compared light and dark black-boned chickens at a single time point after birth [5–8], and one study examined the differences between black-boned and non-black-boned chickens during the embryonic period

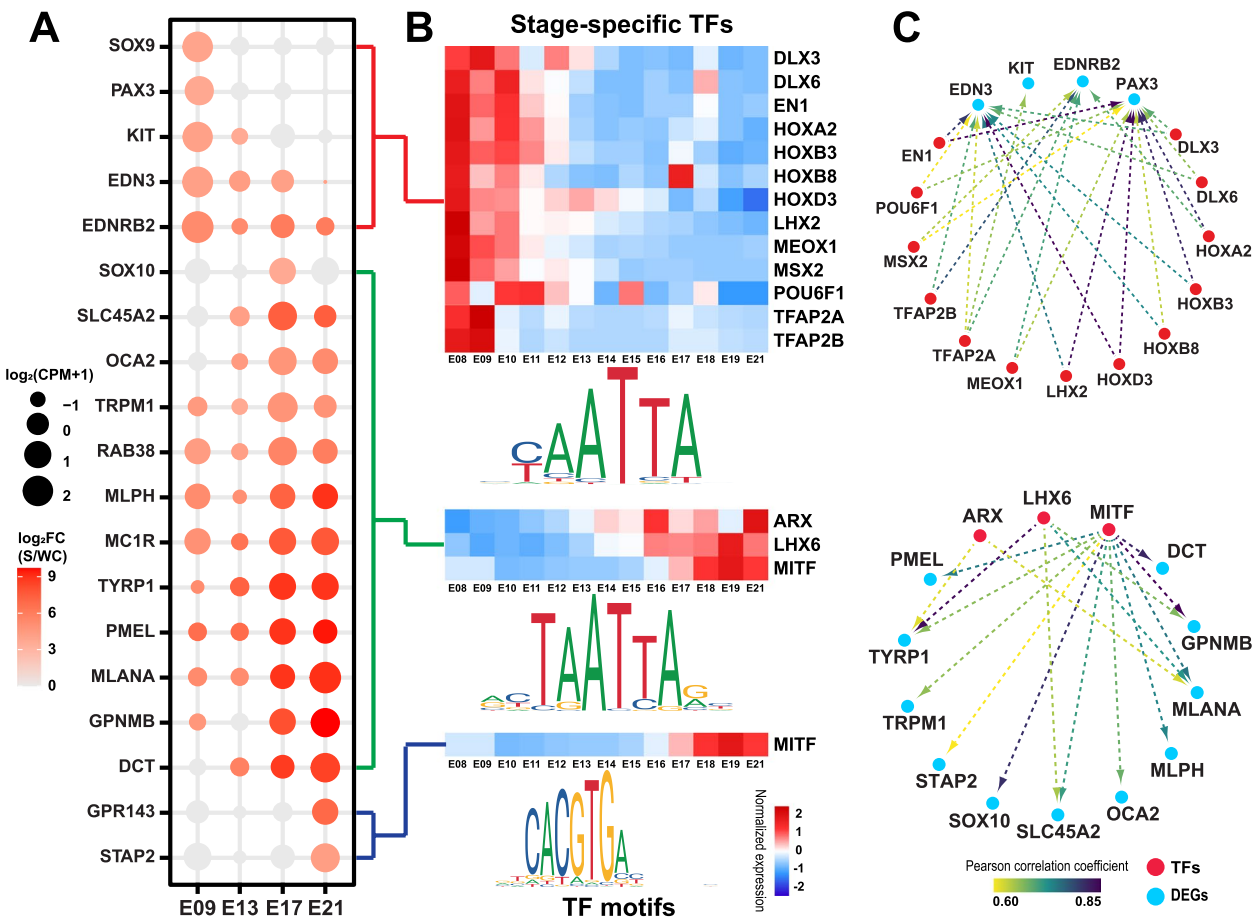

Fig.4 Identification of stage-specific DEGs and TFs with crucial roles in breast muscle melanin deposition process. **A** The expression levels and fold change of stage-specific DEGs at various stages of melanin deposition. The size of circle represents the normalized gene expression level in Silkies and the color of circle represents the fold change between Silkies and Wenchang chickens. **B** The normalized gene expression of TFs significantly enriched in promoters of stage-specific DEGs, and the top representative motif are shown below TFs. **C** The networks of stage-specific DEGs regulated by TFs. The colors of edges are the PCC between stage-specific DEGs and TFs (purple for upregulated; yellow for downregulated). Red circles represent enriched TFs, and blue circles represent stage-specific DEGs

[9]. However, there is no comprehensive understanding of the dynamic changes in the biological processes and regulatory mechanism underlying melanin deposition in skeletal muscle during chicken embryonic development. This study used HPLC technology to accurately quantify the melanin content to determine the dynamic changes and stage division of melanin deposition in breast muscle during embryonic development. According to the changes in melanin content and deposition pattern, the melanin deposition process of breast muscle was divided into five stages, including E08 to E10, E11 to E14, E15 to E16, E17 to E18, and E19 to E21. It was found that the melanin deposition process was closely related to muscle development. At the myoblast stage of E08 to E10, no melanin granules were found in breast muscle, whereas at the myotube stage of E11 to E16, trace amounts of melanin appeared in breast muscle and at the muscle fiber stage of E17 to E21, a large amount of melanin was deposited in breast muscle. The results of HE and FM staining showed that melanin granules accumulated around the blood vessels and traveled along the perimysium into the fasciculus. The HE and FM staining of breast muscle of Silkies after birth found that melanin granules were mainly deposited in endomysium, epimysium and around blood vessels. In the late growth period, melanin granules were mainly deposited around blood vessels and melanin granules within fasciculus were significantly reduced (Fig. S1). It is speculated that melanin granules are mainly produced around blood vessels and migrate into fasciculus and with growth and development, melanin synthesis gradually decreases and only remains around blood vessels.

Muscle development is a dynamic biological process reflected in dynamic changes of gene expression patterns

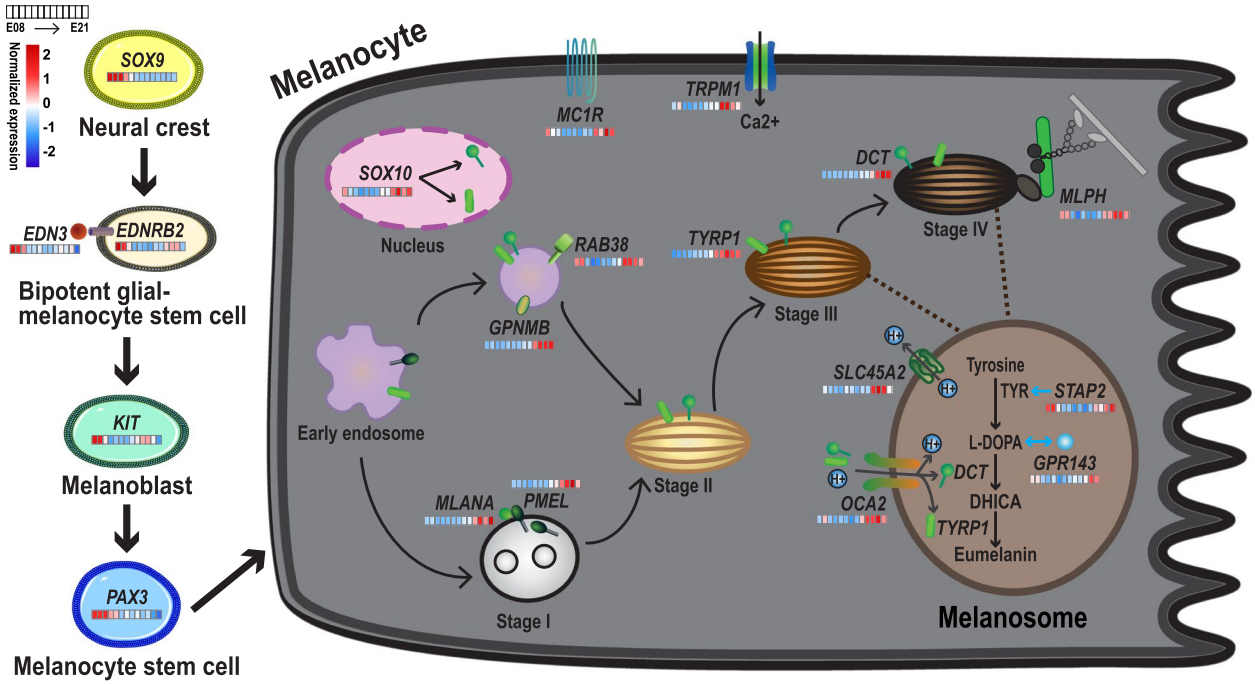

Fig.5 The specific functions and dynamically changing expression levels of stage-specific DEGs in melanin deposition process

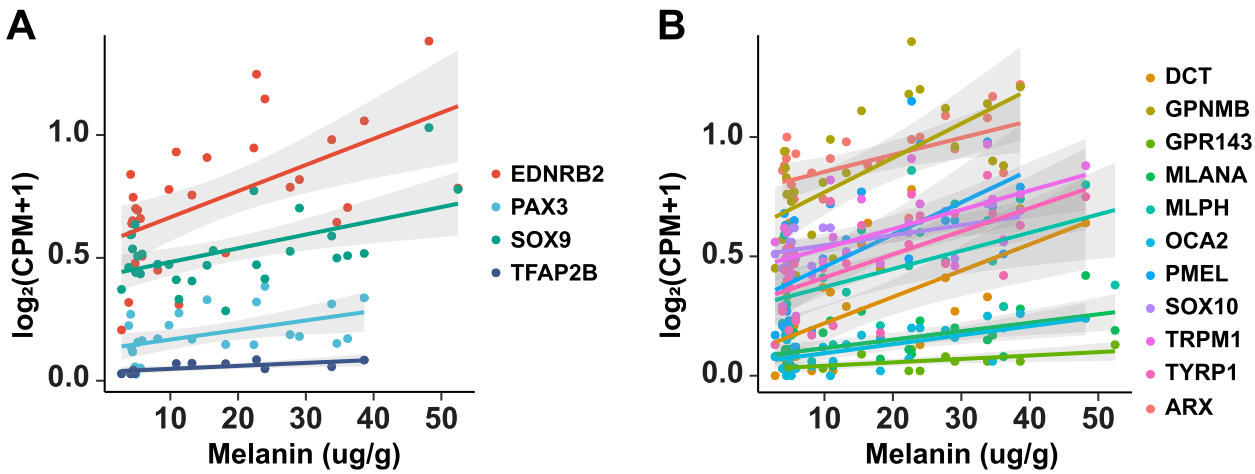

Fig.6 The correlation between the expression of stage-specific DEGs and melanin content in breast muscle of adult Silkies. **A** Key genes with stage-specific expression at E08 to E10. **B** Key genes with stage-specific expression at E17 to E21

at different time points. For this study, a high temporal-resolution dynamic transcriptome landscape of early breast muscle development in Silkies was constructed by sampling 13 time points from E08 to E21. According to the changes in melanin content and deposition pattern during breast muscle development, 13 time points were divided into five periods. Stage-specific expression genes often reflect physiological functions at this stage of development and it was shown that stage-specific PCGs and TFs played critical roles in breast muscle development of chicken embryos. At E08 to E10, a large number of free unfused myoblasts were present, where complex stem cell fate decisions occur and mesodermal cells undergo terminal differentiation and begin to synthesize muscle-specific proteins. The genes *IGF2, FGFR2* and *GATA3* showed stage-specific expression in this period, where *IGF2* promoted proliferation and differentiation of bovine myoblasts [12], *FGFR2* promoted myoblast

proliferation and differentiation and affected skeletal muscle development in chicken [13] and *GATA3* had a role in myoblast differentiation regulation [14]. At E11 to E14, myoblasts were fused in large numbers into multinucleated myotubules and *MYOG* and *SMYD1* showed stage-specific expression in this period. The *MYOG* promoted human myoblast fusion [15] and disruption of MYOG gene in zebrafish can drastically compromise myocyte fusion, significantly reducing myotube sizes [16] and *SMYD1* can accelerate myoblast differentiation and myotube formation [17]. At E15 to E16, myofibrils composed of actin and myosin in the myotubes gradually increased, secondary myotubes formed and *MYOM1* and *XIRP1* showed stage-specific expression in this period. The *MYOM1* helped to cross-link adjacent myosin to form the M-line in myofibrils [18] and played an important role in the assembly and stabilization of myofibrils [19] and *XIRP1* protects actin filaments from depolymerization [20]. At E17 to E18, myotubes rapidly decreased and muscle fibers began to form, with *CAPN3, COL6 A1, COL6 A2, COL6 A3, CSRP3* and *MYH1B* showing stage-specific expression at E17 and E18. The *CAPN3* is essential for the formation of muscle fibers in the embryonic chick [21] and *COL6 A1, COL6 A2* and *COL6 A3* encode collagen type VI, a major microfibrillar component of the extracellular matrix surrounding the muscle fibers. Skeletal muscle fibers of *COL6 A1* knockout mice show signs of degeneration due to a block in autophagy [22] and *CSRP3* plays a crucial role in chicken myofiber composition and affects the distribution of chicken myofiber types by regulating the expression of *MYH1B* [23]. The *ACTA1, KLHL41* and *PPP3 CA* showed stage-specific expression at E19 where *ACTA1* encodes alpha-actin 1, the main constituent of the sarcomeric thin filament, *KLHL41* stabilizes sarcomeres and maintains muscle function by acting as a molecular chaperone [24] and *PPP3 CA* encodes calcineurin Aα, which plays a critical role in controlling skeletal muscle fiber type [25]. At E21, skeletal muscle matures, glycogen metabolism intensifies and mitochondrial metabolism generates ATP to provide energy for muscle fiber contraction, with *PHKG1, PPP1R3 C* and *COX6 A1* showing stage-specific expression in this period. The *PHKG1* is a catalytic subunit of the phosphorylase kinase, which is critical to glycogen degradation [26], PTG encoded by *PPP1R3 C* is a scaffolding protein that targets protein PP1 to glycogen and plays a critical role in glycogen synthesis [27] and *COX6 A1* is a component of mitochondrial respiratory complex IV, so *COX6 A1*-null mice show neurogenic muscular atrophy leading to difficulty walking [28].

This study focused on genes that were specifically expressed in the five stages of breast muscle melanin deposition and differentially expressed between Silkie and Wenchang chickens. The significantly enriched GO terms for these stage-specific DEGs helped the understanding of the overall process of melanin deposition in breast muscle and the physiological changes caused by melanin deposition. All pigmented melanocytes are derived from a group of migratory embryonic cells referred to as the neural crest [29]. The DEGs specifically expressed at E08 to E10 were significantly enriched in neural crest cell migration, indicating that neural crest cell migration and development mainly occurred in the early embryonic stage. The DEGs specifically expressed at E11 to E14 were significantly enriched in angiogenesis and vasoconstriction, which is consistent with the HE and FM staining results that melanin granules mainly accumulate around blood vessels. The DEGs specifically expressed at E17 to E18 were significantly enriched in melanosome assembly and melanin biosynthesis, which was consistent with the result that melanin content significantly increased at this stage. The DEGs specifically expressed at E19 to E21 were significantly enriched in mitochondrial respiratory chain complex, cholesterol homeostasis and removal of superoxide radicals. Existing research demonstrates a direct relationship between cellular melanin content and mitochondrial function [30]. Melanocytes can synthesize cholesterol via HMG-CoA reductase and transport cholesterol using LDL/Apo-B100/LDLR [31]. Melanin has the property of removing superoxide radicals including hydroxyl radicals and superoxide anions [32].

To identify the key genes influencing the final melanin content of breast muscle, this study focused on stage-specific melanin-related DEGs and detected their TFs. ID locus acts upstream of FM locus. So, all birds expressing the FM phenotype are homozygous wild-type *N at the ID locus, or hemizygous in females as ID is located on the Z chromosome. ID mutant control ectopic migration of neural crest cell-derived melanoblasts throughout the body, and FM mutation increasing *EDN3* gene expression was responsible for continued proliferation and maintenance of melanoblasts [2]. ID mutation and its causal gene are still unclear, and it is necessary to identify the ID causal mutation located on the chromosome Z. However, this may require a complete assembled chromosome Z without gap and a segregating population with related phenotypes to perform ID mutation fine mapping, and combine spatial single-cell transcriptome or in situ hybridization analysis to determine the function of causal gene. In our study, *EDN3* and its receptor *EDNRB2* show stage-specific expression from E08 to E10, and their expression in breast muscle of Silkies were significantly higher than that of Wenchang chickens at E09, indicating that the ectopic migration, proliferation and maintenance of neural crest cell-derived melanoblasts into the breast muscle mainly occur at the very early embryonic

stage. In addition, melanocyte stem cell differentiation also occurred at this stage, and were regulated by *SOX9, EDN3, EDNRB2, KIT* and *PAX3*. The *SOX9* is expressed in neural crest cells and promotes their development into melanocytes [33], *KIT* is required for melanoblast differentiation and plays a role in the development of melanocyte stem cells [29] and *PAX3* functions at a nodal point in melanocyte stem cell differentiation [34]. The processes of melanosome assembly and melanin biosynthesis occur centrally at E17 to E21, where *RAB38, PMEL, MLANA* and *GPNMB* are responsible for melanosome assembly. The *RAB38* regulates the proper trafficking of melanosomal cargoes to melanosomes, *PMEL* plays an essential role in the transition from Stage I to Stage II of melanosomes, *MLANA* is involved in melanosome biogenesis by forming a complex with *PMEL* [35] and *GPNMB* shows homology to the *PMEL* precursor and influences the chemical composition of melanosomes [36]. Total number of melanosomes and melanin synthesis were sharply reduced by *GPNMB*-siRNA transfection [37], where *OCA2* and *SLC45 A2* are responsible for regulating the pH of melanosome. The *OCA2* is involved in the transport of tyrosine, the precursor to melanin synthesis, within the melanocyte and regulates the pH of melanosome and the melanosome maturation, *SLC45 A2* acts as proton/glucose exporter which increase luminal pH by decreasing glycolysis and *MLPH* tethers melanosomes to the actin cytoskeleton in melanocytes for transport. The *DCT* and *TYRP1* play direct roles in melanin biosynthesis, where *DCT* catalyzes the conversion of L-dopachrome into 5,6-dihydroxyindole-2-carboxylic acid (DHICA) and *TYRP1* catalyzes the oxidation of DHICA into indole-5,6-quinone-2-carboxylic acid. The *MC1R, TRPM1, STAP2, SOX10 and GPR143* indirectly regulate melanin biosynthesis, where *MC1R* can mediate melanogenesis via regulation of cAMP signaling in melanocytes [38], *TRPM1* forms ion channels associated with melanin content in melanocytes [39], *STAP2* positively regulates the protein levels of tyrosinase, which is the critical and rate-limiting enzyme required for melanogenesis [40], *SOX10* regulate the promoter of *DCT* and *GPR143* is involved in melanosomal biogenesis as a ligand of L-DOPA, a precursor in melanin synthesis.

Conclusions

This study revealed the biological process and regulatory mechanism of melanin deposition in the breast muscle of Silkie chickens through the high temporal-resolution transcriptome landscape across 13 embryonic time points. Based on the dynamic changes of melanin content, the melanin deposition process in breast muscle was accurately divided into five stages as E08 to E10, E11 to E14, E15 to E16, E17 to E18 and E19 to E21. The DEGs between Silkie and Wenchang chickens specifically expressed in five stages revealed the overall process of melanin deposition in breast muscle and suggested that the melanin deposition process was related to angiogenesis, mitochondrial respiration and removal of superoxide radicals. On E08 to E10, three stage-specific DEGs played key roles in neural crest cell migration and melanocyte stem cell differentiation and were regulated by one stage-specific TF. On E17 to E21, 10 stage-specific DEGs played key roles in melanosome assembly and melanin biosynthesis and were regulated by one stage-specific TF. These stage-specific DEGs and TFs significantly affected the melanin content in breast muscle of adult Silkies. This study systematically explored the changing patterns and occurrence periods of melanin abnormal deposition in breast muscle during embryonic development, and reveals the specific biological processes and regulatory genes at each stage. These datasets and findings provided a valuable resource for understanding the biology of melanin abnormal deposition in skeletal muscle.

Materials and methods

Animals and sample collection

Silkie chickens and their fertilized eggs were all descended from the Institute of Animal Sciences (IAS) experimental sites of the Chinese Academy of Agricultural Sciences (CAAS, Beijing, China). The eggs were incubated at 37.8 °C and 55% relative humidity in an automated egg incubator, rotating every 6 h. Thirteen embryonic time points from E08 to E21, and three male Silkie embryos at each time point were used for this study. The embryos were euthanized by cervical dislocation. The sex of Silkie embryos was identified by genomic PCR. The TransDirect® Animal Tissue PCR Kit (TransGen Biotech, China) was used for liver tissue lysis and PCR amplification according to the manufacturer's instructions. The primer sequences of *CHD1* gene are shown in Table S9. The length of PCR products in female embryos was 600 bp and 450 bp, and the length of PCR products in male embryos was 600 bp.

Three hundred Silkie chickens were raised from 1-day-old at the IAS experimental sites of CAAS. These chickens were housed together in the same facility, and they were provided with the same commercial feed and drinking water, allowing them to feed and drink freely. When they reached 24 weeks of age, 30 male Silkies were randomly selected and euthanized by carotid artery bleeding after 12 h of fasting at night.

The intact breast muscle samples from the left and right sides were separated. The left breast muscle samples were snap-frozen in liquid nitrogen for the subsequent transcriptome and melanin content measurement. The right breast muscle samples were used for histological

observation, which were fixed in 4% paraformaldehyde. After embedding in paraffin, 5 μm tissue sections were processed and stained with the FM method for the visualization of melanin distribution. The HE staining was performed according to the classic method [41].

Melanin content measurement

Melanin content was indirectly quantified using 1H-pyrrole-2,3-dicarboxylic acid (PDCA) and 1H-pyrrole-2,3,5-tricarboxylic acid (PTCA), which are the hydrolysates of melanin under alkaline hydrogen peroxide oxidation condition [42]. The breast muscle samples (0.1 g) of Silkie chickens were mixed with 0.5 ml of 30% hydrogen peroxide and 0.5 ml of 2 M ammonium hydroxide. The sample was kept at the bottom of the plastic tube for 8 h at 30 °C. To quench the hydrogen peroxide, 400 μl of 11.3% ammonium sulfite solution was added, then 400 μl of 4 M acetic acid was added to adjust the acidity for the solid-phase extraction (SPE) column (Agela, USA) clean-up. Columns were conditioned with 1 ml methanol and 1 ml ultrapure water. The total sample was then added to the SPE column and allowed to pass through the column under gravity, then 3 ml of water and methanol were added sequentially for washing. The SPE column was then thoroughly dried using a vacuum pump. Elution was carried out with two portions of 1 ml of a 10% (v/v) triethylamine in methanol solution. The eluate was evaporated using nitrogen gas. Dried samples were reconstituted in 1 ml of a methanol solution containing 0.5% formic acid.

The reconstituted sample was analyzed using a QTRAP 6500 LC–ESI–MS/MS system (Sciex, USA) equipped with an ESI Turbo IonSpray interface. The liquid chromatography analysis used a 3 mm × 150 mm ZORBAX column C18 (Agilent, USA) with a mobile phase, A: water (0.1% acetic acid), B: acetonitrile (0.1% acetic acid); gradient program, 2% B at 0 min, 2% B at 1 min, 20% B at 5.6 min, 100% B at 7.0 min, 100% B at 9.4 min, 2% B at 9.6 min, 2% B at 12.0 min, with a flow rate of 0.35 ml/min and a column temperature of 45 °C. The mass spectrometer (MS) parameters were set as source temperature of 500 °C and negative ion spray voltage of (–) 4500 V. For gas I and gas II, the curtain gas was set at 50, 50 and 35 psi, respectively and the collision gas was medium. The multiple reaction monitoring transitions were PTCA 198 to 154 as the quantifier and 198.13 to 110.19 as the qualifier and PDCA 154.13 to 110.13 as the quantifier and 154.13 to 66.15 as the qualifier.

Transcriptome analysis

Total RNA was extracted from breast muscle tissue of Silkie chickens using Trizol reagent. The quality and quantity of all extracted RNA were assessed using Nanodrop and agarose gel electrophoresis. Three micrograms of RNA was used for cDNA library preparation with PrimerScript RT Master Mix RR036 A (Takara, Japan). Library preparations were sequenced on an X-Ten platform (Illumina, USA) and 150-bp paired-end reads were generated. Sequencing adaptors and low-complexity reads were removed using Trimmomatic version 0.36 software [43]. The clean data were mapped to the Gallus gallus reference genome GCA_016699485.1 using TopHat version 2.0.11 software [44]. Read counts of each gene were obtained by running HTSeq version 0.6.1 software [45]. The counts per million (CPM) mapped sequence read for each gene were calculated using edgeR version 3.20.9 packages [46].

The transcriptome data of Wenchang chicken breast muscle were downloaded from NCBI. The accession numbers can be found in BioProject: PRJNA827465.

Statistical analysis

Stage-specific genes (|FoldChange (FC)|≥ 1, false discovery rate (FDR) <0.05) and DEGs (|FC|≥ 1, FDR <0.05) were identified using the R package DESeq2 [47]. Stage-specific genes were identified between one stage and others. Stage-specific DEGs were genes which specifically expressed at a certain stage, and also differentially expressed between Silkie and Wenchang chickens at this stage. Stage-specific genes were separately clustered with the R k-means function where k= 6 within the cluster package according to the Euclidean distance. The gene set enrichment analysis (GSEA) was performed using the R package GSVA, together with the annotated gene sets C5 for Gallus gallus downloaded from the MsigDB database [48]. The GO pathway enrichment analyses were performed using DAVID tools (https://david.ncifcrf.gov/home.jsp). The sequence motif enrichment analysis of promoters of stage-specific genes was conducted by MEME Suite (V 5.5.2) [49], based on the JASPAR (2022) core non-redundant vertebrate motifs from Tomtom [50]. Clustering heatmaps were visualized with the R package pheatmap [51]. The principal component analysis (PCA) plot and bubble chart were visualized with the R package ggplot2 [52]. The regulatory network between TFs and their target genes was visualized using Cytoscape (V 3.8.2).

Supplementary Information

The online version contains supplementary material available at https://doi.org/10.1186/s12864-025-11654-2.

Supplementary Material 1. Fig. S1 The melanin distribution in breast muscle of Silkies at four time points after birth. Dynamic changes in melanin content measured by HPLC. HE staining of breast muscle for transversal sections (magnification: ×20). FM staining of breast muscle for transversal sections (magnification: ×20).

Supplementary Material 2. Fig. S2 Network diagram of stage-specific PCGs regulated by stage-specific TFs. (A-F) represent the regulation of stage-specific PCGs by stage-specific TFs in each cluster 1 to 6, respectively. The blue circles in the center represent enriched TFs. Corresponding biological processes are shown next to stage-specific PCGs with the same color.

Supplementary Material 3. Table S1. Melanin content and proportion of melanin granules in breast muscle during embryonic development.

Supplementary Material 4. Table S2. The Identification and K-means clustering of stage-specific genes.

Supplementary Material 5. Table S3. Motif enrichment analysis for promoters of stage-specific PCGs.

Supplementary Material 6. Table S4. The correlation of TFs and their targeted PGCs in each cluster during breast muscle development.

Supplementary Material 7. Table S5. Stage-specific DEGs between breast muscles of Silkies and Wenchang chickens at each time point.

Supplementary Material 8. Table S6. Motif enrichment analysis for promoters of stage-specific DEGs in breast muscle melanin deposition process.

Supplementary Material 9. Table S7. The correlation of stage-specific DEGs and TFs with crucial roles in breast muscle melanin deposition process.

Supplementary Material 10. Table S8. The correlation between stage-specific DEGs and melanin content in breast muscle.

Supplementary Material 11. Table S9. The primer sequences of CHD1 gene.

Authors' contributions
JZ and YQ designed the research. XY and BM wrote the paper. XY, BM, QZ, YJ, QM and CT collected the data. XY and BM performed the study. XY analyzed data. JZ and CT revised the final manuscript. All authors reviewed the manuscript.

Funding
This work was supported by National Key R&D Program of China [2023YFD1600103]; China Agriculture Research Systems [CARS-40-K11]; Beijing Agriculture Innovation Consortium [BAIC06-2024-G05]; The Chinese Academy of Agricultural Science and Technology Innovation Project [ASTIP-IAS-12].

Data availability
The transcriptome data of Silkie chickens is available from China National Center for Bioinformation and have been assigned BioProject accession PRJCA019528 (https://ngdc.cncb.ac.cn/bioproject/browse/PRJCA019528).

Declarations

Ethics approval and consent to participate
All animal procedures used in this study were approved by the Animal Care and Use Committee of the IAS of the CAAS (IAS2023-108). Experimental procedures and methods were conducted in accordance with approved guidelines to ensure animal welfare.

Consent for publication
Not applicable.

Competing interests
The authors declare no competing interests.

Author details
[1]State Key Laboratory of Animal Nutrition and Feeding, Institute of Animal Sciences, Chinese Academy of Agricultural Sciences, Beijing 100193, China.

Received: 22 April 2024 Accepted: 29 April 2025
Published online: 13 May 2025

References

1. Dubey S, Roulin A. Evolutionary and biomedical consequences of internal melanins. Pigment Cell Melanoma Res. 2014;27(3):327–38.
2. Dorshorst B, Molin A-M, Rubin C-J, Johansson AM, Strömstedt L, Pham M-H, Chen C-F, Hallböök F, Ashwell C, Andersson L. A Complex Genomic Rearrangement Involving the Endothelin 3 Locus Causes Dermal Hyperpigmentation in the Chicken. PLoS Genet. 2011;7(12): e1002412.
3. Li G, Li D, Yang N, Qu L, Hou Z, Zheng J, Xu G, Chen S. A genome-wide association study identifies novel single nucleotide polymorphisms associated with dermal shank pigmentation in chickens. Poult Sci. 2014;93(12):2983–7.
4. Mica Y, Lee G, Chambers Stuart M, Tomishima Mark J, Studer L. Modeling Neural Crest Induction, Melanocyte Specification, and Disease-Related Pigmentation Defects in hESCs and Patient-Specific iPSCs. Cell Rep. 2013;3(4):1140–52.
5. Li D, Wang X, Fu Y, Zhang C, Cao Y, Wang J, Zhang Y, Li Y, Chen Y, Li Z. Transcriptome analysis of the breast muscle of xichuan black-bone chickens under tyrosine supplementation revealed the mechanism of tyrosine-induced melanin deposition. Front Genet. 2019;10:457.
6. Yu S, Wang G, Liao J, Tang M. Transcriptome profile analysis identifies candidate genes for the melanin pigmentation of breast muscle in Muchuan black-boned chicken. Poult Sci. 2018;97(10):3446–55.
7. Dou T, Yan S, Liu L, Wang K, Jian Z, Xu Z, Zhao J, Wang Q, Sun S, Talpur MZ, et al. Integrative analysis of transcriptomics and metabolomics to reveal the melanogenesis pathway of muscle and related meat characters in Wuliangshan black-boned chickens. BMC Genomics. 2022;23(1):173.
8. Xu M, Tang S, Liu X, Deng Y, He C, Guo S, Qu X: Genes influencing deposition of melanin in breast muscle of the Xuefeng black bone chicken based on bioinformatic analysis. Genome 2023.
9. Ji G, Zhang M, Ju X, Liu Y, Shan Y, Tu Y, Zou J, Shu J, Li H, Zhao W. Dynamic Transcriptome Profile Analysis of Mechanisms Related to Melanin Deposition in Chicken Muscle Development. Animals. 2024;14(18):2702.
10. Zhao B, Luo H, He J, Huang X, Chen S, Fu X, Zeng W, Tian Y, Liu S, Li C-j et al: Comprehensive transcriptome and methylome analysis delineates the biological basis of hair follicle development and wool-related traits in Merino sheep. BMC Biology 2021, 19(1):197.
11. Yang Y, Yan J, Fan X, Chen J, Wang Z, Liu X, Yi G, Liu Y, Niu Y, Zhang L, et al. The genome variation and developmental transcriptome maps reveal genetic differentiation of skeletal muscle in pigs. PLoS Genet. 2021;17(11): e1009910.
12. Song C, Yang Z, Jiang R, Cheng J, Yue B, Wang J, Sun X, Huang Y, Lan X, Lei C, et al. lncRNA IGF2 AS Regulates Bovine Myogenesis through Different Pathways. Molecular therapy Nucleic acids. 2020;21:874–84.
13. Chen X, Ouyang H, Wang Z, Chen B, Nie Q: A Novel Circular RNA Generated by FGFR2 Gene Promotes Myoblast Proliferation and Differentiation by Sponging miR-133a-5p and miR-29b-1–5p. In: Cells. vol. 7; 2018.
14. Han S-Z, Gao K, Chang S-Y, Choe H-M, Paek H-J, Quan B-H, Liu X-Y, Yang L-H, Lv S-T, Yin X-J, et al. miR-455-3p Is Negatively Regulated by Myostatin in Skeletal Muscle and Promotes Myoblast Differentiation. J Agric Food Chem. 2022;70(33):10121–33.
15. Zhang H, Wen J, Bigot A, Chen J, Shang R, Mouly V, Bi P: Human myotube formation is determined by MyoD–Myomixer/Myomaker axis. Science Advances, 6(51):eabc4062.
16. Ganassi M, Badodi S, Ortuste Quiroga HP, Zammit PS, Hinits Y, Hughes SM. Myogenin promotes myocyte fusion to balance fibre number and size. Nat Commun. 2018;9(1):4232.
17. Li D, Niu Z, Yu W, Qian Y, Wang Q, Li Q, Yi Z, Luo J, Wu X, Wang Y, et al. SMYD1, the myogenic activator, is a direct target of serum response factor and myogenin. Nucleic Acids Res. 2009;37(21):7059–71.
18. Hang C, Song Y, Li Yn, Zhang S, Chang Y, Bai R, Saleem A, Jiang M, Lu W, Lan F et al: Knockout of MYOM1 in human cardiomyocytes leads to myocardial atrophy via impairing calcium homeostasis. Journal of Cellular and Molecular Medicine 2021, 25(3):1661–1676.
19. Fukuzawa A, Lange S, Holt M, Vihola A, Carmignac V, Ferreiro A, Udd B, Gautel M. Interactions with titin and myomesin target obscurin and obscurin-like 1 to the M-band: implications for hereditary myopathies. J Cell Sci. 2008;121(11):1841–51.
20. Steiner J, Veid C, Lang C: Unique Skeletal Muscle Gene Expression Signature Induced by Acute Alcohol Intoxication in mice. The FASEB Journal 2019, 33(S1):870.874–870.874.

21. de Andrade RI, Corrêa S, Costa ML, Mermelstein C. The scaffolding protein calpain-3 has multiple distributions in embryonic chick muscle cells and it is essential for the formation of muscle fibers. Tissue Cell. 2020;67: 101436.
22. Nair U, Klionsky DJ. Activation of autophagy is required for muscle homeostasis during physical exercise. Autophagy. 2011;7(12):1405–6.
23. Shan Y-j, Ji G-g. Zhang M, Liu Y-f, Tu Y-j, Ju X-j, Shu J-t, Zou J-m: Use of transcriptome sequencing to explore the effect of CSRP3 on chicken myoblasts. J Integr Agric. 2023;22(4):1159–71.
24. Ramirez-Martinez A, Cenik BK, Bezprozvannaya S, Chen B, Bassel-Duby R, Liu N, Olson EN: KLHL41 stabilizes skeletal muscle sarcomeres by nonproteolytic ubiquitination. eLife 2017, 6:e26439.
25. Wan L, Ma J, Xu G, Wang D, Wang N: Molecular Cloning, Structural Analysis and Tissue Expression of Protein Phosphatase 3 Catalytic Subunit Alpha Isoform (PPP3CA) Gene in Tianfu Goat Muscle. In: International Journal of Molecular Sciences. vol. 15; 2014: 2346–2358.
26. Ma J, Yang J, Zhou L, Ren J, Liu X, Zhang H, Yang B, Zhang Z, Ma H, Xie X, et al. A Splice Mutation in the PHKG1 Gene Causes High Glycogen Content and Low Meat Quality in Pig Skeletal Muscle. PLoS Genet. 2014;10(10): e1004710.
27. Zhu X, Yao T, Wang R, Guo S, Wang X, Zhou Z, Zhang Y, Zhuo X, Wang R, Li JZ. IRF4 in skeletal muscle regulates exercise capacity via PTG/glycogen pathway. Advanced Science. 2020;7(19):2001502.
28. Tamiya G, Makino S, Hayashi M, Abe A, Numakura C, Ueki M, Tanaka A, Ito C, Toshimori K, Ogawa N, et al. A Mutation of COX6A1 Causes a Recessive Axonal or Mixed Form of Charcot-Marie-Tooth Disease. The American Journal of Human Genetics. 2014;95(3):294–300.
29. White RM, Zon LI. Melanocytes in Development, Regeneration, and Cancer. Cell Stem Cell. 2008;3(3):242–52.
30. Boulton SJ, Birch-Machin MA. Impact of hyperpigmentation on superoxide flux and melanoma cell metabolism at mitochondrial complex II. FASEB J. 2015;29(1):346–53.
31. Schallreuter KU, Hasse S, Rokos H, Chavan B, Shalbaf M, Spencer JD, Wood JM. Cholesterol regulates melanogenesis in human epidermal melanocytes and melanoma cells. Exp Dermatol. 2009;18(8):680–8.
32. Różanowska M, Sarna T, Land EJ, Truscott TG. Free radical scavenging properties of melanin: Interaction of eu- and pheo-melanin models with reducing and oxidising radicals. Free Radical Biol Med. 1999;26(5):518–25.
33. Cheung M, Briscoe J. Neural crest development is regulated by the transcription factor Sox9. Development (Cambridge, England). 2003;130(23):5681–93.
34. Lang D, Lu MM, Huang L, Engleka KA, Zhang M, Chu EY, Lipner S, Skoultchi A, Millar SE, Epstein JA. Pax3 functions at a nodal point in melanocyte stem cell differentiation. Nature. 2005;433(7028):884–7.
35. Raposo G, Marks MS. Melanosomes — dark organelles enlighten endosomal membrane transport. Nat Rev Mol Cell Biol. 2007;8(10):786–97.
36. Haraszti T, Trantow CM, Hedberg-Buenz A, Grunze M, Anderson MG. Spectral analysis by XANES reveals that GPNMB influences the chemical composition of intact melanosomes. Pigment Cell Melanoma Res. 2011;24(1):187–96.
37. Zhang P, Liu W, Yuan X, Li D, Gu W, Gao T. Endothelin-1 enhances the melanogenesis via MITF-GPNMB pathway. BMB Rep. 2013;46(7):364–9.
38. Ozdeslik RN, Olinski LE, Trieu MM, Oprian DD, Oancea E. Human nonvisual opsin 3 regulates pigmentation of epidermal melanocytes through functional interaction with melanocortin 1 receptor. Proc Natl Acad Sci U S A. 2019;116(23):11508–17.
39. Oancea E, Vriens J, Brauchi S, Jun J, Splawski I, Clapham DE: TRPM1 Forms Ion Channels Associated with Melanin Content in Melanocytes. Science Signaling 2009, 2(70):ra21-ra21.
40. Sekine Y, Togi S, Muromoto R, Kon S, Kitai Y, Yoshimura A, Oritani K, Matsuda T. STAP-2 protein expression in B16F10 melanoma cells positively regulates protein levels of tyrosinase, which determines organs to infiltrate in the body. J Biol Chem. 2015;290(28):17462–73.
41. Fischer AH, Jacobson KA, Rose J, Zeller R: Hematoxylin and eosin staining of tissue and cell sections. Cold spring harbor protocols 2008, 2008(5):pdb-prot4986.
42. Galvan I, Solano F. Bird Integumentary Melanins: Biosynthesis, Forms, Function and Evolution. Int J Mol Sci. 2016;17(4):520.
43. Bolger AM, Lohse M, Usadel B. Trimmomatic: a flexible trimmer for Illumina sequence data. Bioinformatics. 2014;30(15):2114–20.
44. Trapnell C, Pachter L, Salzberg SL. TopHat: discovering splice junctions with RNA-Seq. Bioinformatics. 2009;25(9):1105–11.
45. Anders S, Pyl PT, Huber W. HTSeq—a Python framework to work with high-throughput sequencing data. Bioinformatics. 2015;31(2):166–9.
46. Robinson MD, McCarthy DJ, Smyth GK. edgeR: a Bioconductor package for differential expression analysis of digital gene expression data. Bioinformatics. 2010;26(1):139–40.
47. Love MI, Huber W, Anders S. Moderated estimation of fold change and dispersion for RNA-seq data with DESeq2. Genome Biol. 2014;15(12):550.
48. Subramanian A, Tamayo P, Mootha VK, Mukherjee S, Ebert BL, Gillette MA, Paulovich A, Pomeroy SL, Golub TR, Lander ES, et al. Gene set enrichment analysis: A knowledge-based approach for interpreting genome-wide expression profiles. Proc Natl Acad Sci. 2005;102(43):15545–50.
49. Bailey TL, Johnson J, Grant CE, Noble WS. The MEME suite. Nucleic Acids Res. 2015;43(W1):W39–49.
50. Fornes O, Castro-Mondragon JA, Khan A, van der Lee R, Zhang X, Richmond PA, Modi BP, Correard S, Gheorghe M, Baranašić D, et al. JASPAR 2020: update of the open-access database of transcription factor binding profiles. Nucleic Acids Res. 2020;48(D1):D87–92.
51. Kolde R. Pheatmap: pretty heatmaps. R package version. 2012;1(2):726.
52. Wickham H. Data Analysis. In: Wickham H, editor. ggplot2: Elegant Graphics for Data Analysis. Cham: Springer International Publishing; 2016. p. 189–201.

Publisher's Note